Heliyon 10 (2024) e33090

Contents lists available at ScienceDirect

Heliyon

journal homepage: www.cell.com/heliyon

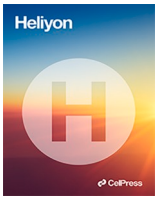

Review article

Machine learning-based diagnosis and prognosis of IgAN: A systematic review and meta-analysis

Kaiting Zhuang [a], Wenjuan Wang [b], Cheng Xu [a], Xinru Guo [b], Xuejing Ren [c], Yanjun Liang [a], Zhiyu Duan [a], Yanqi Song [a], Yifan Zhang [a], Guangyan Cai [a,*]

[a] Department of Nephrology, First Medical Center of Chinese PLA General Hospital, State Key Laboratory of Kidney Diseases, National Clinical Research Center for Kidney Diseases, Beijing Key Laboratory of Kidney Diseases Research, Beijing 100853, China
[b] School of Medicine, Nankai University, Tianjin, 300071, China
[c] Zhengzhou University People's Hospital, Henan Provincial People's Hospital, Henan Key Laboratory of Kidney Disease and Immunology, Academy of Medical Sciences, Zhengzhou University, Zhengzhou, Henan, 450003, China

ARTICLE INFO

Keywords:
Machine learning (ML)
Prognosis
Diagnosis
IgAN
Meta-analysis
Systematic review

ABSTRACT

Purpose: Plenty of studies have explored the diagnosis and prognosis of IgA nephropathy (IgAN) based on machine learning (ML), but the accuracy lacks the support of evidence-based medical evidence. We aim at this problem to guide the precision treatment of IgAN.
Methods: Embase, Pubmed, Cochrane Library, and Web of Science were searched systematically until February 24th, 2024, for publications on ML-based diagnosis and prognosis of IgAN. Subgroup analysis or meta-regression was conducted according to modeling method, follow-up time, endpoint definition, and variable type. Further, the rank sum test was applied to compare the discrimination ability of prognosis.
Results: A total of 47 studies involving 51,935 patients were eligible. Among the 38 diagnostic models, the pooled C-index was 0.902 (95 % CI: 0.878–0.926) in 27 diagnostic models. Of the 162 prognostic models, the C-index for model discrimination of 144 prognostic models was 0.838 (95 % CI: 0.827–0.850) in training. The overall discrimination ability of prognosis was as follows: COX regression > new ML models (e.g. ANN, DT, RF, SVM, XGBoost) > traditional ML models (logistic regression) > Naïve Bayesian network ($P < 0.05$). External validation of IIgAN-RPT in 19 models showed a pooled C-index of 0.801 (95 % CI: 0.784–0.817).
Conclusions: New ML models have shown application values that are as good as traditional ML models, both in diagnosis and prognosis. In addition, future models are desired to use a more sensitive prognostic endpoint (albuminuria), improve predictive ability in moderate progression risk, and ultimately translate into clinically applicable intelligent tools.

1. Introduction

Immunoglobulin A nephropathy (IgAN) is the most prevalent primary glomerulonephritis that coincides with the 'multiple hits' theory and is characterized by the presence of mesangial deposition of IgA [1]. A recent epidemiology study found a 50 % risk of end-stage renal disease (ESRD) in patients with IgAN within 5–10 years [2]. The renal pathological changes of IgAN may predate

* Corresponding author. Department of Nephrology, First Medical Center of Chinese PLA General Hospital, National Key Laboratory of Kidney Diseases, National Clinical Research Center for Kidney Diseases, Beijing Key Laboratory of Kidney Diseases Research, Beijing, 100853, China.
E-mail address: caiguangyan@sina.com (G. Cai).

https://doi.org/10.1016/j.heliyon.2024.e33090
Received 9 August 2023; Received in revised form 4 June 2024; Accepted 13 June 2024
Available online 14 June 2024

functional decline. Therefore, early diagnosis and identification of the progression are essential for developing personalized treatment strategies, facilitating patient-informed clinical decision-making, and guiding the rational recruitment of clinical trial participants.

Numerous researchers have attempted to apply machine learning (ML) to nephropathy, including diagnostic assistance, prognosis, alerting, and guiding treatment in recent years [3]. ML outperforms traditional statistical methods due to its robustness to data noise, ability to learn from multiple data modules, accuracy in identifying key variables, clarity in complex modeling relationships, and improved predictive performance [4]. Recently, Ramspek CL. et al. [5] have conducted a systematic review and meta-analysis of ML in identifying the kidney failure risk in patients with chronic kidney disease (CKD). Nonetheless, different etiologies of CKD may lead to significant heterogeneity in prediction. Therefore, as an important cause of CKD, it is necessary to comprehensively analyze the application of ML in IgAN. Unveiling the predictive performance of ML in IgAN can help guide personalized treatment, determine follow-up frequency, and minimize unnecessary use of immunosuppressants in low-risk patients. Accurate prediction tools are especially important for heterogeneous diseases like IgAN.

Previous studies have demonstrated that ML has ideal application value in the diagnosis and prognosis of IgAN, and it can be used as an auxiliary tool for clinicians. As early as 1998, Geddes, CC. et al. [6] first found that artificial neural networks (ANN) outperformed experienced pathologists in predicting the occurrence of progressive IgAN. However, individual and geographic differences result in heterogeneity in the diagnosis and prediction of IgAN. The inherent complexity and specificity of ML also affect its accuracy in diagnosing IgAN. Therefore, more and better types of ML have been developed to make diagnoses using specific or easily accessible variables. The Oxford Classification of IgAN was separately modeled before it was included as the predictor of the ML model. In this case, the prediction model performed well [7]. In addition, crescent calculators were developed to identify the formation of active crescent [8]. The specific pathological details in IgAN such as immunocomplex deposition are also captured by ML [9]. In addition to diagnosis, ML has been applied for prognosis, complication prediction [10,11], even timing of drug intervention [12], and response to treatment [13]. Several studies have compared the predictive power of multiple model types [14]. IgAN prediction models have been developed in ML prognostic studies that combine genetic, proteomic, imaging, metabolic, and microbiome data and clinical and histopathological information, the widely excavated possibility of urine, serum, and fecal metabolites as modeling variables [15], and the hard endpoints to the composite outcome. Due to the dynamic nature of renal outcomes, prognostic prediction is as challenging as shooting at a moving target. To this end, efforts have been made to develop models to predict the time to ESRD [16–19]. Moreover, to

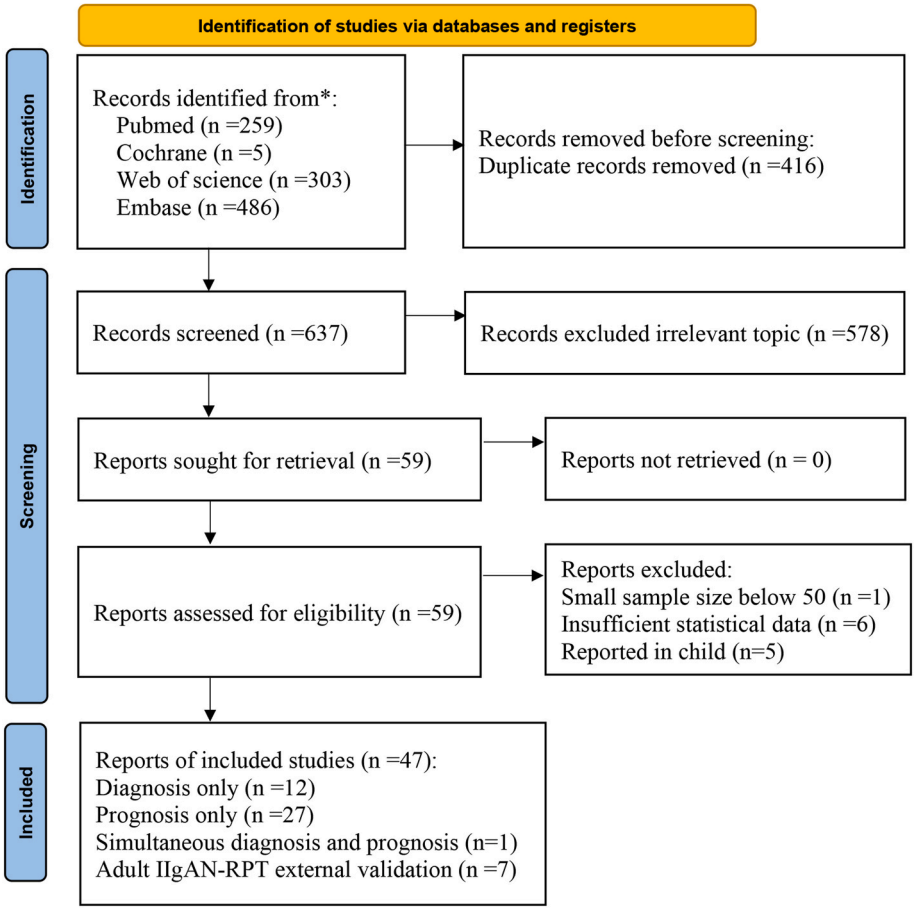

Fig. 1. Flow chart of literature screening.

deal with the difficulty of limited long-term follow-up, long-term risk prediction models have also received attention [20,21].

After exploration for 20 years, nephrologists formally develop an adult International IgAN renal prognosis tool (IIgAN-RPT) in 2019 [22]. The researchers also updated it over time [23] and drew samples from the pooled cohort used in IIgAN-RPT for internal validation [15,24]. Based on this model, a pediatric prognostic model was subsequently established [25]. Although adult IIgAN-RPT has been established [22], its regional applicability remains controversial, and imperfect risk-scoring systems force us to learn from previous models. Thus, this study performed the first comprehensive analysis of ML for the diagnosis and prognosis of IgAN, as well as the external validation of IIgAN-RPT. This will provide evidence-based medical support for the development of precision medicine.

2. Materials and methods

The present study was reported following the Preferred Reporting Guidelines of the Systematic Review (PRISMA 2020) (Table S1). The study protocol has been registered on PROSPERO, and the registration number is CRD42022343310.

2.1. Search strategy

Pubmed, Web of Science, Cochrane, and Embase databases were searched for relevant studies published before June 20, 2022. No restrictions were imposed on region or language. The search terms were designed according to a combination of medical subject headings (MeSH) and entry terms. Based on the two subject words, “ML” and “IgA nephropathy”, the search strings were adjusted for each database. The specific search strategy is displayed in Table S2. In addition, to reduce the risk of missing newly published literature, the search of each database was updated on February 24th, 2024.

2.2. Literature screening

The retrieved articles were imported into Endnote X9 for management. After duplicates were eliminated, the titles and abstracts were scanned to exclude irrelevant studies (Fig. 1).

2.3. Eligibility criteria for meta-analysis

The inclusion criteria were as follows:

(1) The subjects of the diagnostic model were patients with fully recorded predictive variables, while the subjects of the prognostic model were patients with IgAN confirmed by renal biopsy.
(2) RCTs, case-control studies, cohort studies, case-control studies, and case-cohort studies.
(3) An ML model for the diagnosis of IgAN or IgAN renal progression (ESRD and its alternative endpoint) was completely constructed.
(4) Research on different ML methods published based on the same data set.
(5) Literature published in English.

Meanwhile, the following studies were excluded:

(1) Meta-analyses, reviews, guidelines, expert opinions, etc.
(2) Only risk factor analysis was carried out, and no risk model was constructed.
(3) ML model accuracy evaluation indicators (AUC, C-index, sensitivity, specificity, accuracy, recall rate, accuracy rate, confusion matrix, diagnostic 2×2 tables, F1 score, calibration curve) are missing.
(4) Studies with few samples (<50 cases).
(5) Studies that focused only on the validation of a clinical scale.

2.4. Data extraction

Before the meta-analysis, we extracted important statistics, including the total number of samples and the number of events in the training and validation sets, the C-index and their 95 % confidence intervals (95%CI) or standard errors (SE), sensitivity, specificity, accuracy, calibration slope, net reclassification index (NRI), and integrated discrimination improvement (IDI). Two researchers (Kaiting Zhuang and Wenjuan Wang) independently extracted the data and cross-checked their results. If there were any disagreements, a third researcher (Cheng Xu) was invited to assist in the final decision.

2.5. Risk of bias (quality) assessment

The Prediction Model Risk of Bias Assessment Tool (PROBAST) was used to assess the risk of bias in the included studies. The PROBAST tool involves four domains, including participants, predictors, outcomes, and statistical analysis. The overall risk of bias was rated as low when all domains were considered low-risk; otherwise, the overall risk of bias was considered high. Two investigators (Yifan Zhang and Yanjun Liang) independently conducted the risk of bias assessment and cross-checked their results. Any

Table 1
Variable distribution in diagnostic study.

	age	sex	BMI	meanarterialpressure	historyofhypertension	historyofdiabetes	familyhistoryofhematuria	serumIgA	serumIgG	serumIgA/C3ratio	eGFR	creatinine	proteinuria	UPCR	serumalbumin	hematuria	Pathologicimages	otherserumbiomarker	otherurinarybiomarker	microbiome
Gao2011												✓						✓		
Ducher2013	✓	✓			✓	✓	✓	✓			✓		✓			✓				
Takahashi2021																	✓			
Pan2021																	✓			
Park2021	✓	✓		✓							✓			✓					✓	
Hou2022	✓							✓	✓	✓	✓				✓	✓				
Yang2022																	✓			
Zhang, L2021																	✓			
Zhang, D2022																		✓		
Qin2023								✓								✓				
Fan2023																	✓			
Mavrogeorgis2023																				
Fu2024																		✓		

Note: UPCR = urinary protein to creatinine ratio, BMI = body mass index, eGFR = estimated glomerular filtration rate.

disagreements were resolved by discussing them with a third reviewer to reach a consensus (Yanqi Song).

2.6. Data synthesis

We calculated the effect sizes by combining the indicators (C-index, sensitivity, and specificity) for model evaluation of ML. If the C-index lacked a 95 % confidence interval (95 % CI) or standard error (SE) in the included studies, we estimated it according to the following formula proposed by Debray TP et al. [26].

$$\mathrm{SE}(c) \approx \sqrt{\frac{c(1-c)\left[1+\frac{n^*(1-c)}{2-c}+\frac{m^*c}{1+c}\right]}{mn}}$$

n: number of observed events. m: total sample size. $n^* = m^* = \frac{m+n}{2} - 1$. c: C-index.

Given the differences in the variables included in ML models and the inconsistent parameters, a random-effects model was preferable for our meta-analysis. Furthermore, subgroup analyses were performed according to model type, variable type (e.g., including drug use, crescent, pathologic information or not), endpoint definition, and follow-up time. Moreover, in terms of the strengths and weaknesses of model types, the Kruscal-Wallis H rank sum test was adopted to compare the C-index of all types of models. In terms of subgroups with more than 10 models, meta-regression analysis of follow-up time and C-index was performed. This meta-analysis was performed using R4.2.0 (R Development Core Team, Vienna, http://www.R-project.org).

3. Results

3.1. Literature screening

A total of 1053 papers were searched. After excluding papers with irrelevant topics, 1 studies [27] with fewer than 50 cases, 6 [9,15,18,24,28,29] with insufficient statistics, and 5 [30–34] reported in Child were excluded according to a full-text review, the remaining 47 [7,14,20–23,35–75] studies were eligible for meta-analysis. Of the 47 eligible studies, 12 and 27 [7,14,20–23,44–63,74] studies constructed diagnostic and prognostic models, respectively. Additionally, one [70] study constructed models both in diagnosis and prognosis, and another 7 [64–69,75] studies conducted external validation of IIgAN-RPT. The meta-analysis of IgAN diagnosis, IgAN prognosis, and IIgAN-RPT validation involved 7270, 36659, and 8006 patients with 38, 162, and 19 models, respectively. The included studies in the meta-analysis of IgAN diagnosis, IgAN prognosis, and IIgAN-RPT validation were from 6, 20, and 5 countries and were mainly published between 2021 and 2024, 2018 to 2023, and 2020 to 2024, respectively. Notably, the prediction of crescent formation in IgAN has received increasing attention in the last two years.

Table 2
Basic information of included diagnostic study.

Study	Patient source	IgAN No.	Sum	Study design	Validation method	Variable selection	Modeling	Model discrimination
Gao, J.2011	China, USA	120	276	case control	cross validation	U + M	SVM	a, sen, spe
Ducher, M.2013	France	44	149	retrospective cohort	random split	M	The best: BN	sen, spe, C-index
Takahashi, K.2021	Japan	162	422	retrospective cohort	random split	N/A	CNN	sen, spe
Sai Pan2021	China	655	1608	retrospective cohort	random split	M	CNN	a, r, p, F1 score, C-index
Park, S.2021	Korea	201	497	prospective cohort	bootstrap	U + M	LR	C-index
Hou, J.2022	China	212	730	case control	random split	U + M	The best: ANN	C-index, sen, spe
Yang2022	China	51	258	retrospective cohort	random split	N/A	CNN	a, r, p, F1 score, AUC
Zhang, L2021	China	198	623	cross-sectional	random split	M	The best: RF	sen, spe, AUC, a
Zhang, D2022	China	33	53	case control	random split	M	LR	a, r, p, AUC
Qin2023	China	54	120	prospective	random split	U + M	Deep learning	sen, spe, AUC, a
Fan2023	China	186	370	retrospective cohort	random split	N/A	Deep learning	AUC, a, Yoden
Mavrogeorgis2023	Germany	737	1850	retrospective cohort	random split	M	SVM	C-index, a
Fu2024	China	78	314	cross-sectional	random split	N/A	The best: RF	ROC

Note: U = univariable analysis, M = multivariable analysis, SVM=Support Vector Machine, BN=Bayesian Network, CNN=Convolutional Neural Network, LR = Logistic Regression, ANN= Artificial Neural Network, sen = sensitivity, spe = specificity, a = accuracy, r = recall, p = precision.

Table 3
Basic information and methodology of included prognostic study.

Study	EPV	Study Design	Model presentation	Risk stratification		Data processing				Model evaluation		
					Model	missing value	Shrinkage	Variable screen	Validation method	Discrimination	Calibration	Reclassification
Goto2008	11.33	prospective	decision tree	yes, 4 class	The best: DT	multiple impute	N/A	U + M	CV, BT	c	N/A	N/A
Goto2009	31.50	prospective	risk chart	yes, 4 class	COX	N/A	N/A	M	RS, BT	c	N/A	N/A
Xie2012	16.75	retrospective	equation	yes, 3 class	COX	N/A	uniform	U + M	EV	c, sen, spe	N/A	N/A
Tanaka2013	31.60	retrospective	risk chart	no	COX	delete	N/A	U + M	EV	c	Hosmer-Lemeshow test	N/A
Diciolla2015	40.17	prospective	online calculator	yes, 2 class	The best: ANN	delete	uniform	M	CV, post pruning	a, p, r, f	N/A	N/A
Noh2015	17.89	retrospective	N/A	no	The best: LR	delete	N/A	M	RS, BT, EV	c, sen, spe	N/A	N/A
Barbour2016	23.14	prospective	N/A	no	COX	delete	N/A	M	BT	c, IDI	calibration plot	NRI
Liu2017	24.00	retrospective	nomogram	no	COX	N/A	N/A	U + M	EV	c	calibration plot	N/A
Liu, L.2018	19.33	prospective	nomogram	yes, 2 class	COX	delete	N/A	U + M	RS, BT	c	calibration plot	N/A
Liu, Y.2018	1.90	retrospective	N/A	no	RF	delete	N/A	U + M	RS, out of bagging, BT	c, f	N/A	N/A
Xie2018	42.40	retrospective	equation	no	COX	N/A	N/A	U + M	EV	c	N/A	N/A
Zhang2018	30.14	retrospective	nomogram	no	COX	N/A	N/A	U + M	BT	c, sen, spe	N/A	N/A
Han2019	8.68	retrospective	N/A	no	The best: RF	delete	N/A	U + M	CV	a, sen, spe, c	N/A	N/A
Barbour2019	50.36	prospective	online calculator	yes, 4 class	COX	delete	N/A	M	EV	c, IDI	calibration plot	NRI
Chen2019	5.22	retrospective	Risk chart	yes, 4 class	The best: XGB	multiple impute	lasso	U + M	EV	c	Hosmer-Lemeshow test.	N/A
Li2020	unclear	prospective	online calculator	no	XGB	average impute	lasso	U + M	EV	c	N/A	N/A
Yang2020	10.89	prospective	N/A	no	COX	delete	N/A	U + M	EV	c, IDI	N/A	NRI
Schena2021	19.42	retrospective	online calculator	yes, 4 class	ANN	delete	N/A	U + M	CV, RS, EV	c, sen, spe	May-Hosmer test	N/A
Zhai2021	9.20	retrospective	nomogram	yes, 2 class	COX	delete	N/A	U + M	BT	c, a	calibration plot	N/A
Park2021	2.64	prospective	N/A	no	COX	N/A	N/A	U + M	BT	c	N/A	NRI
Barbour2022	36.29	prospective	online calculator	yes, 4 class	COX	multiple impute	N/A	M	RS, BT	c, IDI	ICI, calibration plot	NRI
Haaskjold2022	12.20	retrospective	risk chart	yes, 4 class	COX	N/A	N/A	U + M	BT	c	calibration plot	N/A
Wen2022	13.44	retrospective	N/A	yes, 3 class	COX	delete	N/A	U + M	Unclear	c, IDI	N/A	NRI
Xu2023	11.759	Prospective	decision tree	no	The best: XGBoost	multiple impute	N/A	M	CV	c, sen, spe, AUC	calibration plot	N/A
Haaskjold2023	3.3623	retrospective	decision tree	no	RF	multiple impute	N/A	M	N/A	c	N/A	N/A
Tian2023	19.962	cross-sectional	N/A	no	cox	N/A	N/A	U + M	bootstrap	a, AUC, p, r, F1 score	calibration plot	N/A
Kim2023	8.1824	retrospective	N/A	yes, 3 class	RF	multiple impute	N/A	M	CV	c, sen, spe,	N/A	N/A
Schena2023	11.759	retrospective	online calculator	yes, 3 class	RF	N/A	N/A	M	N/A	sen, spe,	N/A	N/A

Note: EPV = sample size/variable number, SVM = support vector machine, BN = bayesian network, CNN = convolutional neural network, LR = logistic regression, ANN = artificial neural network, COX = cox regression, XGB = eXtreme Gradient Boosting, RF = random forest, DT = decision trees, U = univariable analysis, M = multivariable analysis, sen = sensitivity, spe = specificity, c = C-index, a = accuracy, r = recall, p = precision, f = f-measure, NRI = net reclassification index, IDI = integrated discriminant index, EV = external validation, CV = cross validation, BT = bootstrap, RS = random split.

Table 4
Variable distribution in prognostic study.

	age	sex	race	BMI	MAP/SP/DP	Kidneydiseasestage	immunosuppressant	RASB	statin	tonsillectomy	serumlipid	familyhistory(kidneydisease)	smokinghistory	hypertensionhistory	combinedscore	subtypeofMESTC	necrosisandarteriolelesion	no.ofglomeruli	serumuricacid	Cr	eGFR	Ureanitrogen/proteinuria/UPE	serumalbumin	UPCR	hematuria	hemoglobin	C3	serumGd − IgA1	otherserumbiomarker	otherurinarybiomarker	renalbiomarker
Goto2008					✓										✓							✓	✓		✓						
Goto2009	✓	✓			✓										✓						✓	✓	✓		✓						
Xie2012					✓																✓	✓				✓					
Tanaka2013																✓					✓	✓									
Diciolla2015	✓	✓												✓	✓					✓		✓									
Noh2015	✓	✓									✓		✓			✓		✓			✓					✓					
Barbour2016					✓										✓						✓	✓				✓					
Liu2017					✓											✓						✓									
Liu, L2018															✓				✓		✓	✓									
Liu, Y2018	✓	✓												✓	✓					✓		✓					✓				
Xie2018	✓	✓																			✓	✓				✓					
Zhang2018						✓					✓					✓				✓		✓				✓					
Han2019	✓	✓			✓	✓	✓	✓						✓	✓				✓	✓	✓	✓	✓		✓						
Barbour2019	✓	✓	✓	✓	✓		✓	✓							✓						✓	✓									
Chen2019	✓	✓		✓	✓		✓	✓	✓	✓	✓	✓		✓	✓		✓		✓	✓	✓	✓	✓		✓						
Li2020	✓	✓		✓	✓		✓	✓	✓	✓	✓	✓		✓	✓		✓		✓	✓	✓	✓	✓		✓						
Yang2020	✓	✓	✓	✓	✓		✓	✓							✓						✓	✓					✓		✓		
Park2021	✓	✓			✓		✓	✓							✓						✓			✓					✓		
Schena2021	✓	✓					✓	✓						✓	✓					✓		✓									
Zhai2021														✓		✓				✓						✓		✓			
Barbour2022					✓																✓	✓									
Haaskjold2022															✓																
Wen2022	✓	✓			✓		✓								✓						✓	✓									✓
Xu2023	✓				✓											✓			✓		✓						✓				
Haaskjold2023																✓					✓	✓		✓							
Tian2023														✓		✓						✓									
Kim2023																✓															
Schena2023							✓	✓								✓					✓	✓									

Note: UPE = urinary protein excretion, SP = systolic pressure, DP = diastolic pressure, MAP = mean arterial pressure, RASB = renin-angiotensin system inhibitor.

3.2. Characteristics of the included studies

We have shown the distribution of variables (Table 1) and the specific characteristics (Table 2) of the 13 diagnostic studies. Of the 13 diagnostic studies, 4 [36,40,42,72] compared the predictive performance of different ML methods. In addition, 4 [39,41,71,73] of the included diagnostic studies explored digital pathology.

The basic information and methodology of the 27 prognostic studies are shown in Table 3, independent external validation was performed in 10 prognostic studies [14,21,22,50,51,53,55,58,60,61]. Among them, three studies [16,17,19] also made Time-to-ESRD predictions, which was helpful for dynamically adjusting clinical decision-making. We have shown the distribution of predictors across studies (Table 4) and sorted the top 20 variables (Fig. 2). It's worth noting that three studies [20,21,53] introduced new pathological variables (tubular necrosis and arteriole lesion) into modeling. Six studies [47,51,70,76–78] of them added additional variables after the introduction of IIgAN-RPT, and the study [51] that included urine biomarkers and serum Gd-IgA1 achieved the highest NRI (0.82 [0.50–1.14]). Table 5 shows the basic information about the external validation of IIgAN-RPT. Two studies [65,75]pointed out the shortcomings of IIgAN-RPT for moderate-risk patients.

3.3. Risk of bias assessment

The risk of bias scores for the diagnosis and prognosis of IgAN, as well as the validation of IIgAN-RPT are shown in Fig. 3a, b, and 3c, respectively. Except for the subjects, applicability items in the others showed a high overall bias. Diagnostic studies were all single-center studies, lacked model calibration, and did not process missing values. Besides, there are several shortcomings in the methodology of prognostic studies. The inevitable use of single-factor analysis to screen predictive factors is one of the data processing defects. Only three prognostic studies [23,53,63] processed missing values of original data by using multiple imputations, and only 3 studies [59,70,79] performed dimension reduction analysis. Overall, 14 prognostic studies [22,23,45–50,53,57,59,61–63] used risk stratification of patients with IgAN and found that ML models could only accurately identify high-risk patients in most cases.

3.4. Meta-analysis

Our meta-analysis was divided into three parts: diagnosis of IgAN, prognosis of IgAN, and external validation of the IIgAN-RPT. Among the 38 diagnostic models, 27 provided a C-index, and 15 provided sensitivity and specificity. The pooled C-index of the 27 diagnostic models was 0.902 (95 % CI: 0.878–0.926) in the training set and 0.851 (95 % CI: 0.808–0.894) in the validation set (Fig. 4). The overall sensitivity and specificity were 0.82 (95 % CI: 0.78–0.86) and 0.81 (95%CI: 0.71–0.88) in the training set, and 0.82 (95 % CI: 0.78–0.86) and 0.81 (95 % CI: 0.71–0.88) in the validation set, respectively (Fig. S1). Subgroup analysis according to model types and variables showed that the C-index of ANN was up to 0.966 and the sensitivity was 0.85. Diagnostic models based solely on pathological variables had similar predictive abilities to those based on the combination of clinical parameters and biomarkers.

In addition, there were 162 prognostic models included in the meta-analysis of prognosis. The meta-analysis showed that the available C-index was pooled to be 0.838 (95 % CI: 0.827–0.850) in the training cohort (Fig. 5) and 0.817 (95 % CI: 0.801–0.833) in the validation cohort (Fig. S2). The overall sensitivity and specificity of models that provide sensitivity and specificity were 0.81 (95 % CI:

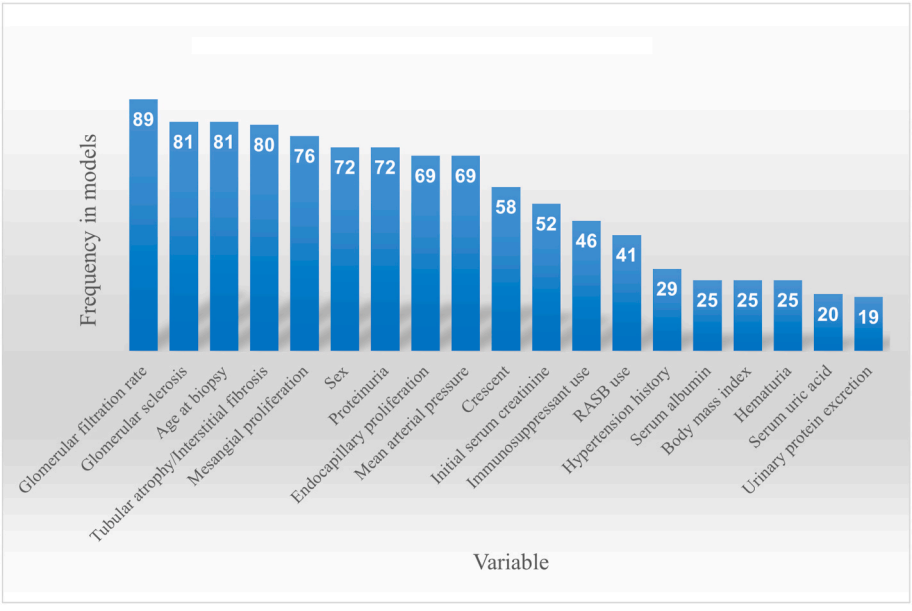

Fig. 2. Top 20 variables in prognostic models.

Table 5
External validation of IIgAN-RPT.

Study	Patient source	Multi racial	Time	EPV	Total No.	Study design	Overfitting solution	Risk stratification	Model evaluation		
									Discrimination	Calibration	Reclassification
Zhang, J.2020	China	no	2.4 y	13.29	1373	retrospective	bootstrap	yes, 4 class	C-index	Calibration plot	NRI, IDI
Zhang, Y.2020	China, Argentina	yes	3.8 y	12.93	1275	prospective	N/A	yes, 4 class	C-index	Calibration plot	N/A
Ouyang, Y.2021	China	no	2.5 y	20.57	2300	prospective	N/A	yes, 2 class	C-index	Calibration plot	NRI
Hwang, D.2021	Korea	no	3.6 y	3.79	545	retrospective	N/A	no	C-index	Calibration plot	NRI, IDI
Papasotiriou2022	Greece	no	8.5 y	3.79	264	prospective	N/A	yes, 4 class	C-index	Calibration slope	N/A
Joo,Y. S.2022	Korea	no	3.8 y	25.21	2064	retrospective	bootstrap	no	C-index	Calibration plot	NRI, IDI
Hu2024	China	no	5.1 y	10.27	185	retrospective	N/A	yes, 4 class	C-index	Calibration plot	N/A

Note: NRI = net reclassification index, IDI = integrated discriminant index, EPV=Sum/variable number.

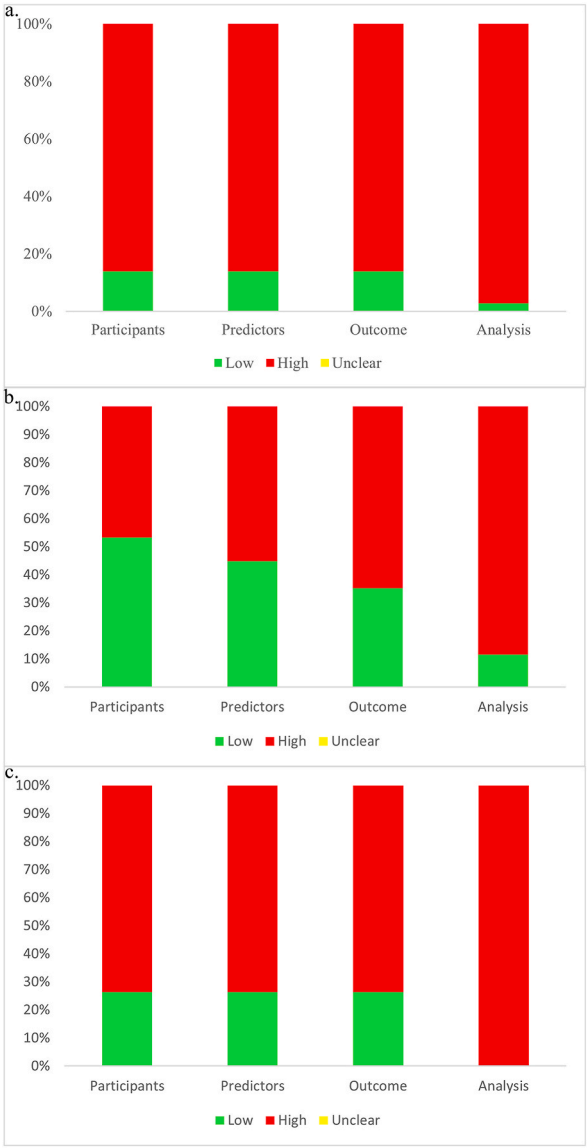

Fig. 3. Risk of bias assessment (a) diagnosis (b) prognosis (c) external validation of IIgAN-RPT.

0.76–0.85) and 0.87 (95 % CI: 0.83–0.90) in the training set (Fig. S3), and 0.88 (95 % CI: 0.78–0.93) and 0.88(95%CI: 0.82–0.92) in the validation set (Fig. S4). The 87 survival models (COX regression) had a C-index of 0.826 (95 % CI: 0.815–0.837) in the training set and 0.828 (95 % CI: 0.810–0.845) in the validation set, indicating that survival models had favorable discriminative ability. In the rank sum test for non-survival models (Fig. 6), the present study revealed that the logistic regression model (C-index = 0.840 (95 % CI: 0.785–0.989)) did not outperform other ML methods except the Naïve Bayesian model (C index = 0.653 (95 % CI: 0.543–0.763)) ($P < 0.05$). Subgroup analysis of variable composition found that the models with higher performance often included pathological variables and did not contain immunosuppressant (IS) or renin-angiotensin system blocker (RASB). More specifically, in the training set, the C-index of biomarker-based models was significantly lower than that of the models based on clinical parameters + pathologic information or clinical parameters + pathologic information + biomarkers, indicating the necessity of introducing other variables into prediction models. According to the subgroup analysis with a 5-year cut-off and the time-dependent meta-regression analysis (Figs. S5–9), the model's efficiency did not change over time either in overall estimation or subgroup of more than 10 models (cox regression and random forest model).

The meta-analysis of the external validation of IIgAN-RPT (19 models) showed a pooled C-index of 0.801 (95 % CI: 0.784–0.817) (Table S3). Whether the modeling variable included race or not made no statistical difference in the C-index between the two subgroups. Three studies [65,67,68]verified that the model's performance was improved after race was included in the modeling variables, and their NRI was 0.52 (95 % CI: 0.33–0.72), 0.13 (95 % CI: 0.08–0.29), and 0.49 (95%CI: 0.41–0.59), respectively. In addition,

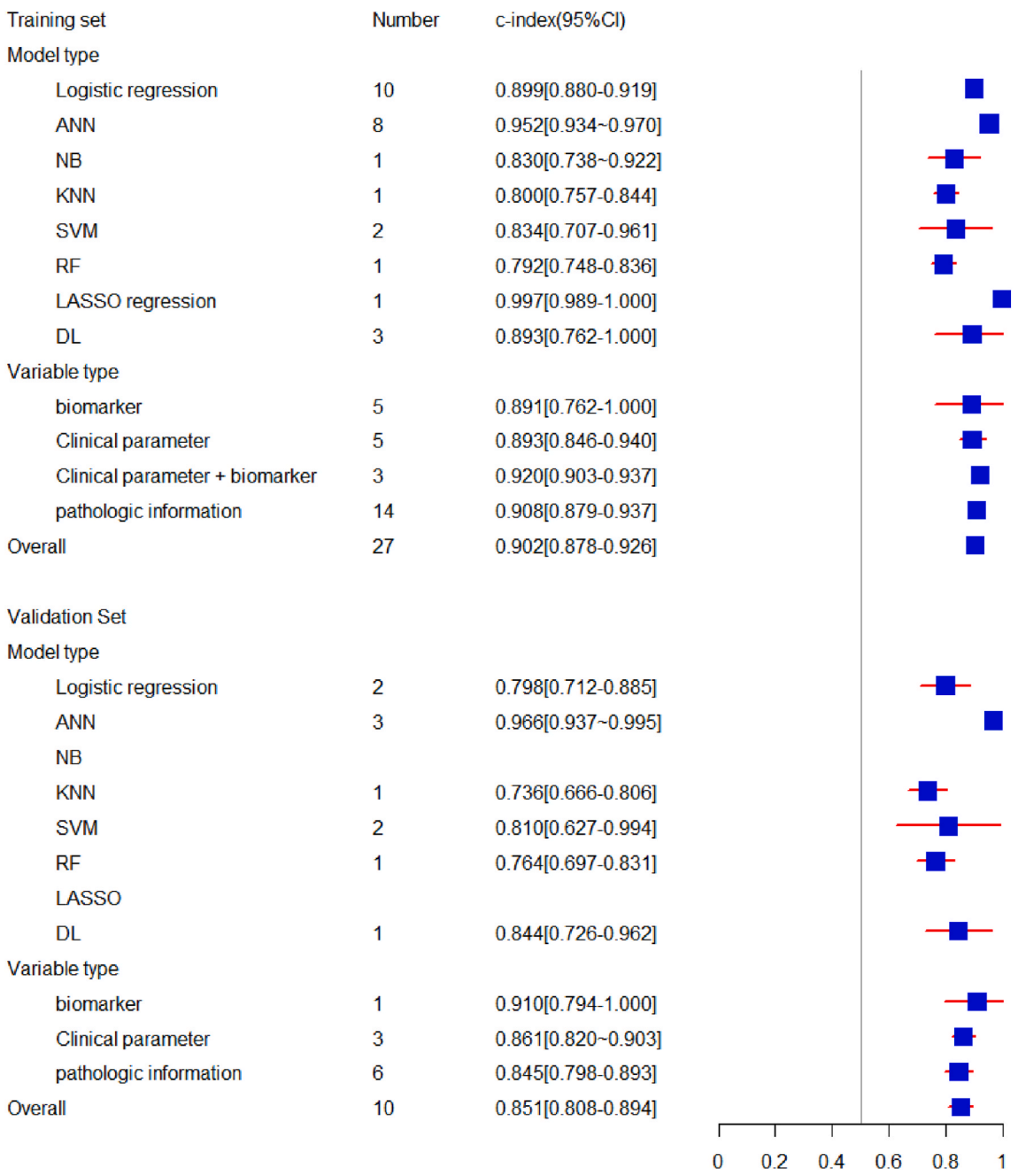

Fig. 4. Forest plot of C-index in diagnostic study (training and validation set).

the Cox regression prognostic models (C index = 0.826 (95 % CI: 0.815–0.837)) that were created formerly were not superior to the COX regression-based international tool (IIgAN-RPT) in 2019.

4. Discussion

4.1. Principal findings

Collectively, ML models showed favorable performance in the diagnosis and prognosis of IgAN. Except for the Naïve Bayesian model, new ML methods were superior to traditional ML methods in terms of prognosis. Predicting smaller details of IgAN, such as crescent activity, also yielded great performance. Previously constructed prognostic models were not superior to IIgAN-RPT. However, due to racial homogeneity in the external validation population of IIgAN-RPT, its generalization remained limited.

Subgroup	Number	c-index(95%CI)
Model type		
Cox regression	90	0.826[0.815~0.837]
Logistic regression	9	0.840[0.785~0.894]
Decision tree	4	0.849[0.812~0.886]
SVM	7	0.854[0.790~0.918]
ANN	6	0.858[0.824~0.893]
RF	19	0.989[0.853~0.924]
KNN	1	0.946[0.927~0.965]
NB	2	0.653[0.543~0.763]
XGBoost	6	0.871[0.845~0.897]
Variable inclusion of using immunosuppressive agents		
No	78	0.837[0.817~0.857]
Yes	49	0.842[0.829~0.856]
Variable inclusion of using RASB		
No	99	0.832[0.812~0.851]
Yes	45	0.853[0.839~0.867]
Variable inclusion of crescent		
No	93	0.844[0.828~0.859]
Yes	51	0.829[0.818~0.840]
Variable composition		
Clinical parameter	23	0.806[0.772~0.840]
biomarker	8	0.775[0.704~0.845]
Clinical parameter + biomarker	9	0.801[0.759~0.843]
Clinical parameter+pathologic information	78	0.861[0.849~0.872]
Clinical parameter+pathologic information+biomarker	17	0.819[0.793~0.845]
pathologic information	8	0.847[0.767~0.927]
pathologic information+biomarker	1	0.850[0.755~0.945]
Variable type		
Exclude pathologic information	40	0.799[0.773~0.824]
Include pathologic information	104	0.852[0.840~0.864]
FollowTime		
~5 Year	54	0.816[0.795~0.837]
5 Year~	90	0.852[0.841~0.862]
Endpoint definition		
decrease in eGFR > 50% or ESRD	42	0.833[0.819~0.846]
ESRD	50	0.883[0.867~0.899]
doubling in sCr or ESRD	3	0.848[0.790~0.906]
decrease in eGFR > 40%(or 30%) or ESRD	49	0.790[0.753~0.827]
Overall	144	0.838[0.827~0.850]

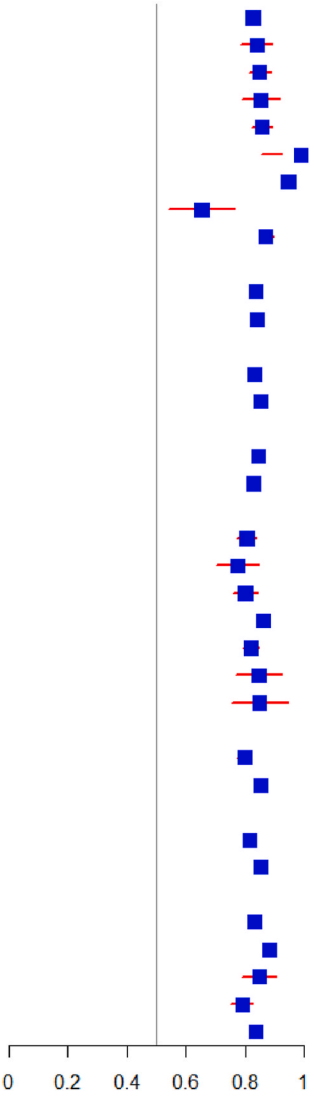

Fig. 5. Forest plot of C-index in prognostic study (training set).

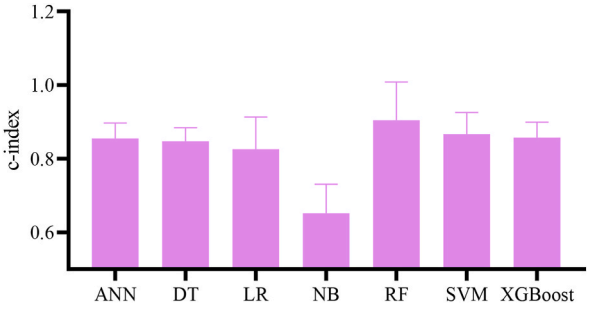

Fig. 6. Rank sum test for non-survival prognostic models.

4.2. Diagnostic ability in IgAN

The diagnostic meta-analysis of IgAN indicated that ANN seemed to be an ideal model for IgAN diagnosis, with acceptable sensitivity. However, due to the limited number and heterogeneity of the included studies, its value needs to be further explored. Subgroup analysis showed that the prediction power of the models based on clinical parameters and biomarkers was similar to those based only on pathological information (>0.9). Their similar prediction power suggests that the models based on clinical parameters and biomarkers have the potential as a diagnostic alternative for healthcare facilities without renal biopsy capability, which needs to be widely validated. The application of ML to digital pathology is an auxiliary means of pathological diagnosis. The technique can automatically quantify glomerular injury and pick up details missed by the naked eye, thereby saving manpower and time and improving diagnostic accuracy. Additionally, image texture segmentation and 3D reconstruction are useful for accurately identifying higher-level features, and avoiding interference caused by inconsistent slice staining. Despite the high accuracy of deep learning models, they have not been applied to practical work, and their translational research deserves attention.

4.3. Prognostic ability in IgAN

IgAN patients have a much lower proteinuria threshold associated with eGFR loss (1 g/d) than most other kidney diseases (3.5 g/d), which makes it unique. Therefore, proteinuria may be a more sensitive endpoint of renal progression than ESRD. This finding is underpinned by the meta-analysis of Inker, L. A. et al. [80]. Proteinuria has been used as an endpoint in clinical trials [81]. Recently, two prognostic studies [45,46] of IgAN considered proteinuria as an outcome definition in ML. However, due to the limited number of studies, we could not determine the utility of proteinuria in the outcome definition.

The predictive value for outcome events is controversial among various ML methods. Our meta-analysis unveiled the performance of different models as follows: COX regression > new ML models (e.g., ANN, DT, RF, SVM, XGBoost) > logistic regression > NB. The meta-analysis of prognosis shows that the discrimination ability of RF and KNN is greater than 0.9, significantly higher than that of COX regression. Seemingly, RF and KNN are the most accurate in prognosis without regard to the occurrence time, but their sensitivity, which is more important for non-survival models, is not better than that of COX regression. Time considerations are particularly important in chronic diseases, and COX regression can handle missing records during follow-up [82]. Hence, survival models (COX regression) are still our first choice. In addition, although traditional ML models (logistic regression) can visualize risk equations and nomograms, which is convenient to apply, new ML methods with higher discrimination ability are of great importance for us to apply to clinical work.

4.4. Variable analysis in prognosis

For ML in clinical practice, predictors are the key to accuracy improvement. At present, the modeling variables in ML for IgAN mainly include clinical parameters, pathologic information, and biomarkers. Unlike diagnostic models, prognostic models should consider clinical variables that change over time to update the prediction. Another notable clinical variable is the treatment history. Current models still cannot adequately predict the effects of IS and RASB on prognosis. Moreover, tonsillectomy, an immunological intervention, was only included as a variable in two studies [21,53]. The effect of these interventions on renal outcomes remains controversial and needs to be further explored.

The crescent, a newly added pathological variable in the updated Oxford classification [83], showed no significant improvement in model performance. This result is consistent with the latest authoritative study [23]. This may be attributable to racial differences and the fact that most crescents occur in the early stage of IgAN. However, a multi-center, high-quality study [84] confirmed its prognostic value of the crescents. Hence, it is necessary to explore a modeling method suitable for the updated Oxford classification. Of concern, 3 studies [8,85,86] reported the prediction of crescent formation in IgAN. The C-index for prediction of crescent activity in IgAN was up to 0.976 [86]. These models that accurately identify the crescent are preferred before the crescent is included as a prognostic variable.

For the biomarkers, subgroup analysis showed a significant increase in specificity, but the sensitivity remained almost unchanged. This finding indicates that existing biomarkers cannot meet the demand for improving discrimination. A urine test is advisable because it is completely non-invasive, and some glomerular sediments are excreted into urine. Furthermore, components encapsulated in urinary exosomes are stable for prediction due to the escape of bio-enzymatic degradation. Candidate biomarkers include pathogenesis-related complement systems (C3, C5, galactose-deficient IgA1) [87,88], amino acid, microbes, humoral morphological features (e.g., macrophage count), and inflammatory markers (e.g., microhematuria). In the absence of medication history, biomarkers such as urinary MMP-7 with stable predictive accuracy regardless of intervention [51] may help in decision-making. In a word, minimally invasive, efficient, and easy-to-collect markers are preferable.

4.5. Temporal analysis and external validation of prognostic models

Longer time frames are critical for assessing slow-progressing diseases such as IgAN. Due to the limitation of irregular outpatient visits, it is often challenging to conduct long follow-up visits as required. Therefore, it is important to determine the long-term predictive power in prognostic models. In our study, neither meta-regression nor subgroup analysis showed a decline in the prognostic ability over time, which was consistent with the findings in a recent authoritative study [23]. Specifically, IIgAN-RPT was validated one year after the biopsy, and no decline in model performance was observed. Similarly, Schena, FP et al. [50] reported no difference in the dynamic discrimination of ESRD one year and two years after biopsy. These results suggest that prognostic models can still be

applied to long-term forecasting of IgAN.

The external validation of IIgAN-RPT reported a relatively well-discriminant ability but limited in number. In addition, inconsistent treatment measures in different countries (such as the widespread use of tonsillectomy in Japan) might result in risk underestimation. Furthermore, due to the limited number, there is a need to develop models that add genetic variables and validate international pediatric models. Therefore, it is essential to develop tailored models for different populations and improve the generalization.

4.6. Strength and limitation

This is the first meta-analysis on the application of ML in IgAN, including the studies on diagnosis, prognosis, and IIgAN-RPT validation. Moreover, our analysis pointed out the methodological deficiencies in the included studies, which can help subsequent studies construct more reliable models that apply to a variety of clinical settings. Nonetheless, this study has several limitations. Above all, the confidence interval of the C-index of some models is unknot clear, or a complete diagnostic 2×2 table cannot be obtained. Therefore, we only reviewed them, which may bias our meta-analysis results. Secondly, the risk of bias in the included studies was high, which is almost inevitable given the rigorous requirements for the use of existing quality assessment tools to evaluate the quality of ML-related studies.

4.7. Future direction

Above all, raw data processing needs to be optimized, such as handling missing values through patient similarity learning and dimensionality reduction analysis based on unsupervised learning. Aiming at the problems of overfitting, inconvenient use, and weight enlargement of tightly-correlated variables caused by excessive modeling variables, interaction tests or covariate screening can be applied to combine or select them. Additionally, in most studies, only NRI was used to assess the improvement of models that added new predictors to the IIgAN-RPT, whereas IDI, a more accurate indicator, was rarely used. It is essential to address potential errors in physician-generated data and the challenges in processing unstructured data. A favorable prediction model should consider both sensitivity and specificity. Furthermore, external validation of pediatric international prognosis tools needs to be extended. In addition to immunosuppressants, the history of tripterygium glycosides should also be checked.

5. Conclusion

ML can help physicians to diagnose IgAN and assess the subsequent prognosis. Expanding the application of three-dimensional reconstruction techniques in diagnostic models, using albuminuria as a more sensitive prognostic endpoint, enhancing moderate-risk prognosis, extending the racial validation scope and pediatric validation of international tools, and translating the model into clinical calculators will be the future direction.

Funding support

The Natural Science Foundation of China (NSFC) (82170686), Grant for GYC (22KJLJ001).

Data availability statement

Data sharing is not applicable to this article as no datasets were generated or analyzed during the current study.

CRediT authorship contribution statement

Kaiting Zhuang: Writing – original draft, Conceptualization. **Wenjuan Wang:** Methodology. **Cheng Xu:** Investigation, Formal analysis. **Xinru Guo:** Writing – review & editing. **Xuejing Ren:** Resources. **Yanjun Liang:** Investigation, Formal analysis. **Zhiyu Duan:** Writing – review & editing. **Yanqi Song:** Resources. **Yifan Zhang:** Investigation, Formal analysis. **Guangyan Cai:** Supervision, Funding acquisition.

Declaration of competing interest

The authors declare that they have no known competing financial interests or personal relationships that could have appeared to influence the work reported in this paper.

Acknowledgements

None.

Appendix A. Supplementary data

Supplementary data to this article can be found online at https://doi.org/10.1016/j.heliyon.2024.e33090.

References

[1] J. Barratt, J. Feehally, IgA nephropathy, J. Am. Soc. Nephrol. 16 (7) (2005) 2088–2097.
[2] J.C. Rodrigues, M. Haas, H.N. Reich, IgA nephropathy, Clin. J. Am. Soc. Nephrol. 12 (4) (2017) 677–686.
[3] Q. Yuan, et al., Role of artificial intelligence in kidney disease, Int. J. Med. Sci. 17 (7) (2020) 970–984.
[4] Q. Li, et al., Machine learning in nephrology: scratching the surface, Chin Med J (Engl) 133 (6) (2020) 687–698.
[5] C.L. Ramspek, et al., Towards the best kidney failure prediction tool: a systematic review and selection aid, Nephrol. Dial. Transplant. 35 (9) (2020) 1527–1538.
[6] C.C. Geddes, et al., An artificial neural network can select patients at high risk of developing progressive IgA nephropathy more accurately than experienced nephrologists, Nephrol. Dial. Transplant. 13 (1) (1998) 67–71.
[7] S.J. Barbour, et al., The MEST score provides earlier risk prediction in lgA nephropathy, Kidney Int. 89 (1) (2016) 167–175.
[8] Q. Zhang, et al., Crescent calculator: a webtool enabling objective decision-making for assessment of IgA nephropathy immune activity throughout the disease course, Clin. Chim. Acta 555 (2024) 117783.
[9] Y. Chen, et al., VGG16-based intelligent image analysis in the pathological diagnosis of IgA nephropathy, Journal of Radiation Research and Applied Sciences 16 (3) (2023).
[10] Y.H. Geng, et al., Established the first clinical prediction model regarding the risk of hyperuricemia in adult IgA nephropathy, Int. Urol. Nephrol. 55 (7) (2023) 1787–1797.
[11] R.B. Wei, et al., Nomogram prediction model for renal anaemia in IgA nephropathy patients, Open Med. 16 (1) (2021) 718–727.
[12] Y. Gu, et al., Syndrome differentiation of IgA nephropathy based on clinicopathological parameters: a decision tree model, Evid. base Compl. Alternative Med. 2017 (2017).
[13] T. Chen, et al., Identification and external validation of IgA nephropathy patients benefiting from immunosuppression therapy, EBioMedicine 52 (2020) 102657.
[14] J. Noh, et al., Machine learning models and statistical measures for predicting the progression of IgA nephropathy, Int. J. Software Eng. Knowl. Eng. 25 (5) (2015) 829–849.
[15] Y.L. Haaskjold, et al., Validation of two IgA nephropathy risk-prediction tools using a cohort with a long follow-up, Nephrol. Dial. Transplant. 38 (5) (2023) 1183–1191.
[16] F.P. Schena, et al., Development and testing of an artificial intelligence tool for predicting end-stage kidney disease in patients with immunoglobulin A nephropathy, Kidney Int. 99 (5) (2021) 1179–1188.
[17] J. Xie, et al., Kidney failure risk prediction equations in IgA nephropathy: a multicenter risk assessment study in Chinese patients, Am. J. Kidney Dis. 72 (3) (2018) 371–380.
[18] F. Pesce, et al., Clinical decision support system for end-stage kidney disease risk estimation in IgA nephropathy patients, Nephrol. Dial. Transplant. 31 (1) (2016) 80–86.
[19] M. Diciolla, et al., Patient classification and outcome prediction in IgA nephropathy, Comput. Biol. Med. 66 (2015) 278–286.
[20] Y.L. Haaskjold, et al., Long-term follow-up of IgA nephropathy: clinicopathological features and predictors of outcomes, Clin Kidney J 16 (12) (2023) 2514–2522.
[21] Y. Li, et al., An interpretable machine learning survival model for predicting long-term kidney outcomes in IgA nephropathy, AMIA Annu Symp Proc 2020 (2020) 737–746.
[22] S.J. Barbour, et al., Evaluating a new international risk-prediction tool in IgA nephropathy, JAMA Intern. Med. 179 (7) (2019) 942–952.
[23] S.J. Barbour, et al., Application of the international IgA nephropathy prediction tool one or two years post-biopsy, Kidney Int. 102 (1) (2022) 160–172.
[24] R. Ebbestad, M. Sanaei Nurmi, S. Lundberg, Long-term outcomes of patients with IgA nephropathy categorized by the international IgAN risk prediction tool and by the degree of hematuria at diagnosis, Nephron 146 (6) (2022) 573–583.
[25] S.J. Barbour, et al., Updating the international IgA nephropathy prediction tool for use in children, Kidney Int. 99 (6) (2021) 1439–1450.
[26] T.P. Debray, et al., A framework for meta-analysis of prediction model studies with binary and time-to-event outcomes, Stat. Methods Med. Res. 28 (9) (2019) 2768–2786.
[27] H. Kataoka, et al., Time series changes in pseudo-R2 values regarding maximum glomerular diameter and the Oxford MEST-C score in patients with IgA nephropathy: a long-term follow-up study, PLoS One 15 (5) (2020).
[28] A. Jaugey, et al., Deep learning automation of MEST-C classification in IgA nephropathy, Nephrol. Dial. Transplant. 38 (7) (2023) 1741–1751.
[29] F. Cai, et al., Systematic microbiome dysbiosis is associated with IgA nephropathy, Microbiol. Spectr. 11 (3) (2023) e0520222.
[30] P. Zhang, R.Q. Wang, N.F. Shi, IgA nephropathy prediction in children with machine learning algorithms, Future Internet 12 (12) (2020).
[31] I. Klimek, et al., Glomerular basement membrane thinning in children: a morphometric assessment, AQCH (Anal. Quant. Cytol. Histol.) 28 (5) (2006) 269–280.
[32] D.J. Ying, et al., External validation of the pediatric international IgA nephropathy prediction tool in a central China cohort, Clin. Exp. Nephrol. 28 (1) (2023) 59–66.
[33] J.M. Zhou, et al., Urinary epidermal growth factor predicts complete remission of proteinuria in Chinese children with IgA nephropathy, Pediatr. Res. 94 (2) (2023) 747–755.
[34] X. Yu, et al., Validation of the children international IgA nephropathy prediction tool based on data in Southwest China, Front Pediatr 11 (2023) 1183562.
[35] E. Mavrogeorgis, et al., Urinary peptidomic liquid biopsy for non-invasive differential diagnosis of chronic kidney disease, Nephrol. Dial. Transplant. 39 (3) (2024) 453–462.
[36] X. Fu, et al., Metabolomics study reveals blood biomarkers for early diagnosis of chronic kidney disease and IgA nephropathy: a retrospective cross-sectional study, Clin. Chim. Acta 555 (2024) 117815.
[37] X. Qin, et al., Development of a novel combined nomogram model integrating deep learning radiomics to diagnose IgA nephropathy clinically, Ren. Fail. 45 (2) (2023) 2271104.
[38] D. Zhang, et al., LC-MS/MS based metabolomics and proteomics reveal candidate biomarkers and molecular mechanism of early IgA nephropathy, Clin. Proteonomics 19 (1) (2022) 51.
[39] C.K. Yang, et al., Glomerular disease classification and lesion identification by machine learning, Biomed. J. 45 (4) (2022) 675–685.
[40] J. Hou, et al., A noninvasive artificial neural network model to predict IgA nephropathy risk in Chinese population, Sci. Rep. 12 (1) (2022) 8296.
[41] K. Takahashi, et al., The resolution of immunofluorescent pathological images affects diagnosis for not only artificial intelligence but also human, Journal of Nephropathology 10 (3) (2021).
[42] M. Ducher, et al., Comparison of a Bayesian network with a logistic regression model to forecast IgA nephropathy, BioMed Res. Int. 2013 (2013) 686150.
[43] J. Gao, et al., Identification of potential predictors for subtype IgA nephropathy through analyses of blood biochemical indicators, Clin. Chim. Acta 412 (5–6) (2011) 441–445.
[44] L.L. Xu, et al., Machine learning in predicting T-score in the Oxford classification system of IgA nephropathy, Front. Immunol. 14 (2023) 1224631.
[45] F.P. Schena, et al., Post-hoc analysis of a tool to predict kidney failure in patients with IgA nephropathy, J. Nephrol. 36 (2) (2023) 451–461.
[46] Y. Kim, et al., Machine learning-based 2-year risk prediction tool in immunoglobulin A nephropathy, Kidney Res. Clin. Pract. (2023). Published online October 27.
[47] L. Wen, et al., Renal megalin mRNA downregulation is associated with CKD progression in IgA nephropathy, Am. J. Nephrol. 53 (6) (2022) 481–489.
[48] Y.L. Haaskjold, et al., Utilizing the MEST score for prognostic staging in IgA nephropathy, BMC Nephrol. 23 (1) (2022) 26.
[49] Y. Zhai, et al., Elevated serum chloride levels contribute to a poor prognosis in patients with IgA nephropathy, J Immunol Res 2021 (2021) 3598135.
[50] F.P. Schena, et al., Development and testing of an artificial intelligence tool for predicting end-stage kidney disease in patients with immunoglobulin A nephropathy, Kidney Int. 99 (5) (2021) 1179–1188.
[51] X. Yang, et al., Urinary matrix metalloproteinase 7 and prediction of IgA nephropathy progression, Am. J. Kidney Dis. 75 (3) (2020) 384–393.

[52] X. Han, et al., Random forest can accurately predict the development of end-stage renal disease in immunoglobulin a nephropathy patients, Ann. Transl. Med. 7 (11) (2019) 234.
[53] T. Chen, et al., Prediction and risk stratification of kidney outcomes in IgA nephropathy, Am. J. Kidney Dis. 74 (3) (2019) 300–309.
[54] L. Zhang, X. Zhuang, X. Liao, A proposed Oxford classification-based clinicopathological nomogram for predicting short-term renal outcomes in IgA nephropathy after acute kidney injury, Eur. J. Intern. Med. 52 (2018) 60–66.
[55] J. Xie, et al., Kidney failure risk prediction equations in IgA nephropathy: a multicenter risk assessment study in Chinese patients, Am. J. Kidney Dis. 72 (3) (2018) 371–380.
[56] Y. Liu, et al., Prediction of ESRD in IgA nephropathy patients from an asian cohort: a random forest model, Kidney Blood Press. Res. 43 (6) (2018) 1852–1864.
[57] L.L. Liu, et al., Development and assessment of a predictive nomogram for the progression of IgA nephropathy, Sci. Rep. 8 (1) (2018) 7309.
[58] J. Liu, et al., Development and validation of a prognostic nomogram for IgA nephropathy, Oncotarget 8 (55) (2017) 94371–94381.
[59] M. Diciolla, et al., Patient classification and outcome prediction in IgA nephropathy, Comput. Biol. Med. 66 (2015) 278–286.
[60] S. Tanaka, et al., Development and validation of a prediction rule using the Oxford classification in IgA nephropathy, Clin. J. Am. Soc. Nephrol. 8 (12) (2013) 2082–2090.
[61] J. Xie, et al., Predicting progression of IgA nephropathy: new clinical progression risk score, PLoS One 7 (6) (2012) e38904.
[62] M. Goto, et al., A scoring system to predict renal outcome in IgA nephropathy: a nationwide 10-year prospective cohort study, Nephrol. Dial. Transplant. 24 (10) (2009) 3068–3074.
[63] M. Goto, et al., Risk stratification for progression of IgA nephropathy using a decision tree induction algorithm, Nephrol. Dial. Transplant. 24 (4) (2009) 1242–1247.
[64] L. Hu, et al., External validation of the international prognosis prediction model of IgA nephropathy, Ren. Fail. 46 (1) (2024) 2313174.
[65] Y.S. Joo, et al., External validation of the international prediction tool in Korean patients with immunoglobulin A nephropathy, Kidney Res Clin Pract 41 (5) (2022) 556–566.
[66] Y. Ouyang, et al., A validation study comparing risk prediction models of IgA nephropathy, Front. Immunol. 12 (2021) 753901.
[67] D. Hwang, et al., Validation of an international prediction model including the Oxford classification in Korean patients with IgA nephropathy, Nephrology 26 (7) (2021) 594–602.
[68] Y. Zhang, et al., External validation of international risk-prediction models of IgA nephropathy in an asian-caucasian cohort, Kidney Int Rep 5 (10) (2020) 1753–1763.
[69] J. Zhang, et al., External validation of the international IgA nephropathy prediction tool, Clin. J. Am. Soc. Nephrol. 15 (8) (2020) 1112–1120.
[70] S. Park, et al., Comprehensive metabolomic profiling in early IgA nephropathy patients reveals urine glycine as a prognostic biomarker, J. Cell Mol. Med. 25 (11) (2021) 5177–5190.
[71] Z. Fan, et al., Artificial intelligence can accurately distinguish IgA nephropathy from diabetic nephropathy under Masson staining and becomes an important assistant for renal pathologists, Front. Med. 10 (2023) 1066125.
[72] L. Zhang, et al., Preliminary study on the application of renal ultrasonography radiomics in the classification of glomerulopathy, BMC Med. Imag. 21 (1) (2021) 115.
[73] S. Pan, et al., Multi-task learning-based immunofluorescence classification of kidney disease, Int. J. Environ. Res. Publ. Health 18 (20) (2021).
[74] Z.Y. Tian, et al., Prognostic value of low-density lipoprotein cholesterol in IgA nephropathy and establishment of nomogram model, Front. Endocrinol. 14 (2023) 1037773.
[75] M. Papasotiriou, et al., Validation of the international IgA nephropathy prediction tool in the Greek registry of IgA nephropathy, Front. Med. 9 (2022) 778464.
[76] H. Dai, et al., Tubular decoy receptor 2 as a predictor of prognosis in patients with immunoglobulin A nephropathy, Clin Kidney J 14 (5) (2021) 1458–1468.
[77] I. Pawluczyk, et al., A pilot study to predict risk of IgA nephropathy progression based on miR-204 expression, Kidney Int Rep 6 (8) (2021) 2179–2188.
[78] M. Rudnicki, et al., Urine proteomics for prediction of disease progression in patients with IgA nephropathy, Nephrol. Dial. Transplant. 37 (1) (2021) 42–52.
[79] T. Di Noia, et al., An end stage kidney disease predictor based on an artificial neural networks ensemble, Expert Syst. Appl. 40 (11) (2013) 4438–4445.
[80] L.A. Inker, et al., Association of treatment effects on early change in urine protein and treatment effects on GFR slope in IgA nephropathy: an individual participant meta-analysis, Am. J. Kidney Dis. 78 (3) (2021) 340–349.e1.
[81] A. Thompson, et al., Proteinuria reduction as a surrogate end point in trials of IgA nephropathy, Clin. J. Am. Soc. Nephrol. 14 (3) (2019) 469–481.
[82] R.L. Prentice, S. Zhao, Regression models and multivariate life tables, J. Am. Stat. Assoc. 116 (535) (2021) 1330–1345.
[83] H. Trimarchi, et al., Oxford classification of IgA nephropathy 2016: an update from the IgA nephropathy classification working group, Kidney Int. 91 (5) (2017) 1014–1021.
[84] M. Haas, et al., A multicenter study of the predictive value of crescents in IgA nephropathy, J. Am. Soc. Nephrol. 28 (2) (2017) 691–701.
[85] Z. Lin, et al., Nomogram for the prediction of crescent formation in IgA nephropathy patients: a retrospective study, BMC Nephrol. 24 (1) (2023) 262.
[86] X. Qin, et al., A novel clinical-radiomic nomogram for the crescent status in IgA nephropathy, Front. Endocrinol. 14 (2023) 1093452.
[87] Z. Moldoveanu, et al., Patients with IgA nephropathy have increased serum galactose-deficient IgA1 levels, Kidney Int. 71 (11) (2007) 1148–1154.
[88] H. Suzuki, et al., Galactose-deficient IgA1 as a candidate urinary polypeptide marker of IgA nephropathy? Dis. Markers 2016 (2016) 7806438.